Direct measurement of the $^{16}O(\alpha,\gamma)^{20}Ne$ reaction at $E_{c.m.} = 2.43$ MeV and 1.69 MeV

U. Hager,[1,*] L. Buchmann,[2] B. Davids,[2] J. Fallis,[2] U. Greife,[1] D. A. Hutcheon,[2] D. Irvine,[3] D. Ottewell,[2] A. Rojas,[2] S. Reeve,[2] and C. Ruiz[2]

[1]*Colorado School of Mines, Golden, Colorado, USA*

[2]*TRIUMF, Vancouver, Canada V6T 2A3*

[3]*McMaster University, Hamilton, Ontario, Canada*

(Received 21 March 2012; revised manuscript received 12 September 2012; published 5 November 2012)

In stars, ^{16}O represents the endpoint of the helium burning sequence due to the low rate of $^{16}O(\alpha,\gamma)^{20}Ne$. We present a new direct measurement of the total cross section of $^{16}O(\alpha,\gamma)^{20}Ne$ at $E_{c.m.} = 1.69$ MeV employing the DRAGON recoil separator. In addition, the branching ratios and strength of the $E_{c.m.} = 2.426$ MeV 3^- resonance were determined.

DOI: 10.1103/PhysRevC.86.055802 PACS number(s): 26.20.Fj, 25.55.−e, 98.80.Ft, 97.10.Cv

I. INTRODUCTION

Steady-state stellar helium burning produces mainly ^{12}C via the triple-α process at typical temperatures of 0.1–0.3 GK. This reaction can in principle be followed by further α-capture reactions. However, the $^{16}O(\alpha,\gamma)^{20}Ne$ reaction is very weak at these temperatures (effective energy for this reaction $E_{c.m.} \approx 0.3$ MeV) due to the lack of a suitable resonance in ^{20}Ne, as shown in Fig. 1. The 2^- state inside the Gamow window is of unnatural parity and therefore cannot be populated by this reaction. The dominant way for the reaction to proceed at astrophysically relevant energies is via nonresonant direct capture (DC), either into the ground state, or through the first excited state at 1.6 MeV. However, in the experimentally accessible energy regimes resonances and their interference with each other and the DC process need to be taken into account. Therefore, R-matrix calculations based on known resonances have been performed [1]. These calculations identify energies where DC makes a significant contribution to the total cross section even at higher center-of-mass energies. These measurements around $E_{c.m.} = 1.7$ MeV and $E_{c.m.} = 2.35$ MeV can serve as tests for the R-matrix parametrizations as they lie near the S factor minimum between resonances (cf. Fig. 12 in Ref. [1]). Additionally, the inverse $^{20}Ne(\gamma,\alpha)^{16}O$ reaction is important in neon burning at temperatures of about 1.7 GK [2]. Its rate can be calculated from the $^{16}O(\alpha,\gamma)^{20}Ne$ rate using the detailed balance theorem [3].

A theoretical evaluation of the $^{16}O(\alpha,\gamma)^{20}Ne$ rate in the semimicroscopic orthogonality condition model (OCM) was conducted by Langanke [4], predicting a direct capture S factor of $S_{DC} = 2.3$ MeVb at $E_{c.m.} = 300$ keV. The DC rate was measured by Hahn *et al.* [5] in inverse kinematics, using an ^{16}O beam on a windowless gas target. They determined the S factor for capture to the ground state to be $S_0 = 0.26 \pm 0.07$ MeVb for $E_{c.m.} = 1.7$–2.35 MeV. The S_2 contribution to the first excited state was not measured, but an upper limit was calculated for the total nonresonant S factor. Using theoretical predictions for the branching ratios and the energy dependence, an estimate for the total S factor of $S(300\,\text{keV}) = 0.7 \pm 0.3$ MeVb at the astrophysically interesting energy was given. In a comment on the measurements of Hahn *et al.*, Baye *et al.* [6] suggest the results obtained in Ref. [5] at $E_{c.m.} = 2.3$ MeV and 2.35 MeV should be remeasured. They suspect that the calculated S factor is probably too low, and the recommended S factor should be multiplied at least by a factor 2.

The $^{16}O(\alpha,\gamma)^{20}Ne$ DC rate has twice been measured at the Stuttgart Dynamitron [7,8]. In addition, both times the strengths and branching ratios of several resonances were determined. The reaction was measured in normal kinematics, using a windowless gas target and HPGe detectors to detect the prompt γ rays. The first measurement by Knee [7] could only determine an upper limit for the S factor in the minima between the resonances. For the direct capture into the ground state an upper limit of $S_0 \leqslant 0.92$ MeVb was found, and for the first excited state $S_2 \leqslant 2.45$ MeVb. The total S factor is given as $S_{tot} \leqslant 3.37$ MeVb. During the second measurement, Mayer [8] extracted a value for DC to the first excited state of $S_2 = 0.69 \pm 0.30$ MeVb. For DC to the ground state, an upper limit of $S_0 \leqslant 0.2$ MeVb was determined, and a total S factor including resonance contributions at 300 keV of $S_{tot} = 4.2 \pm 2.1$ MeVb was recommended.

Using the data presented in Ref. [8] and new measurements of the resonances at $E_{c.m.} = 0.891 - 1.995$ MeV, Costantini *et al.* [1] conducted an R-matrix analysis of the $^{16}O(\alpha,\gamma)^{20}Ne$ cross section. They assumed the decay through the first excited state to contribute $S_2/S_{DC} = 75(10)\%$ at the astrophysically relevant $E_{c.m.} = 300$ keV, and give a total S factor at that energy of $S(300\,\text{keV}) = 1.9$ MeVb.

Due to the low reaction cross section at the energies where a significant DC contribution is expected, and the relatively low efficiency of germanium detectors at high γ energies, most recent measurements determined only the S_2 component through the first excited state in ^{20}Ne, with the S_0 component to the ground state derived from theory. On the other hand, Ref. [5] measured only the S_0 component using a NaI detector coupled to a recoil separator. The first measurement of the total S factor was recently carried out at DRAGON [9] at $E_{c.m.} = 2.26$ MeV, finding good agreement both with the measurement of the S_0 component by Hahn *et al.* [5] at the same energy, and with the R-matrix calculation of the total S factor by Costantini *et al.* [1].

*uhager@mines.edu

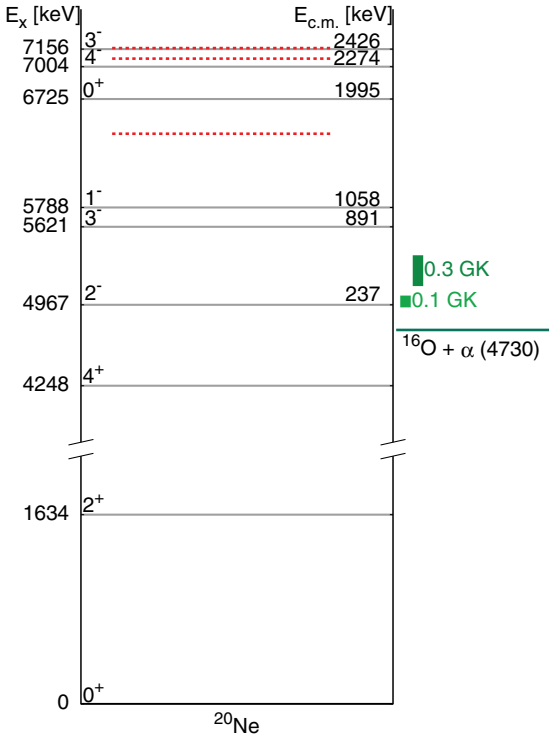

FIG. 1. (Color online) Energy levels in ^{20}Ne. On the right hand side, Gamow windows corresponding to 0.1 GK and 0.3 GK are shown. The dashed, red lines indicate the energies discussed in the present work.

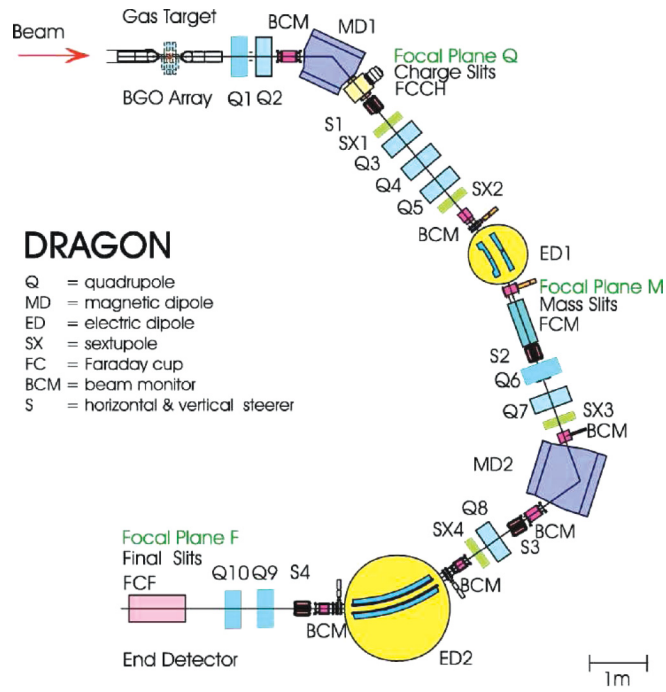

FIG. 2. (Color online) Schematic view of the DRAGON facility.

In this work, we present a direct measurement of the ^{16}O(α,γ)^{20}Ne cross section at $E_{\text{c.m.}} = 1.69$ MeV, between the 1^- resonance at $E_x = 5788$ keV and the 0^+ resonance at $E_x = 6725$ keV. This energy was chosen to minimize resonant contributions, while still having a sufficiently high rate to enable determination of the S_0 and S_2 contributions. In addition, a measurement of the ^{16}O(α,γ)^{20}Ne cross section at the $E_{\text{c.m.}} = 2.43$ MeV resonance was performed and the branching ratios and resonance strength determined. A third measurement was done at $E_{\text{c.m.}} = 2.35$ MeV, on the low-energy edge of the $E_{\text{c.m.}} = 2.43$ MeV resonance. These data points constitute an experimental test of the recent comprehensive R-matrix predictions published in Ref. [1].

II. EXPERIMENTAL PROCEDURE

The measurements were conducted in inverse kinematics at the DRAGON recoil separator [10], located at the ISAC facility at TRIUMF, Vancouver, Canada. A schematic view of the DRAGON facility is shown in Fig. 2. The ^{16}O beam was produced by the Supernanogan off-line ion source [11]. The DRAGON windowless gas target was filled with ^{4}He maintained at a central pressure within 3% of 7.7 Torr; the effective target length was 12.3(5) cm [10]. The DRAGON target was surrounded by an array of 30 bismuth germanate (BGO) γ-ray detectors in a tight geometry. These were calibrated using the 6.13 MeV γ rays emitted by a ^{244}Cm-^{13}C source and adjusting their high-voltage PMT biases until the source peak was aligned in all detectors. Given the resolution of the BGO array (about 24% at 660 keV for the whole array), this calibration with the assumption of linearity is sufficient for the purpose of this work. The geometry of the BGO array enabled determination of the resonance position along the target axis [12]. In order to suppress background, the ^{20}Ne ions produced in the reaction were detected in coincidence with γ events in the BGO array, after separation from the beam using a two-stage electromagnetic separator with an angular acceptance of 21 mrad for reactions at the center of the target. At the energies discussed in this work, the ^{16}O(α,γ)^{20}Ne reaction cone angle is 12–13 mrad, assuming the worst case of a γ decay directly to the ground state of ^{20}Ne.

At the focal plane, an ionization chamber (IC) [13] was used to detect ^{20}Ne recoils from the reaction. Its segmented anode enabled stopping power measurements and thus particle identification (PID). In addition, two MCPs (microchannel plates) upstream of the ionization chamber were used to measure the time-of-flight (TOF) across the 59 cm distance between them [14]. The IC was used to determine the efficiency for both MCPs together. During the present work the efficiency was 98(2)%. The transmission through the MCP TOF setup was 85(5)%. The beam suppression capabilities of the MCPs are illustrated in Fig. 3. As an additional PID parameter, the time-of-flight through the separator was used to identify valid recoil coincidence events, as shown in Fig. 4.

Since the separator transmits ^{20}Ne recoils of only one charge state, determining the total cross section requires knowledge of the distribution of charge states of neon after passing through helium. This distribution was measured using a beam of ^{20}Ne, also from the Supernanogan. The reaction measurements were performed in charge state 4^+, which gave the best suppression of ^{16}O 'leaky' beam. When using higher

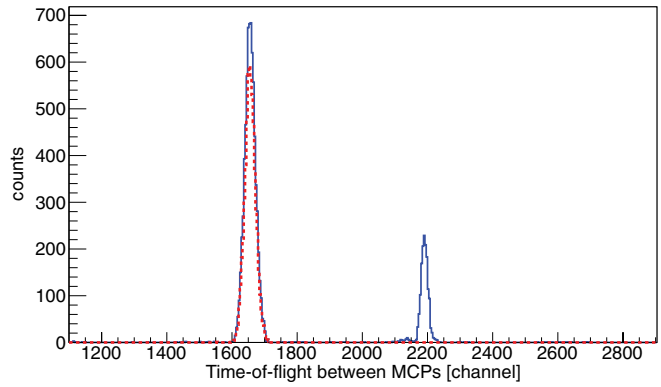

FIG. 3. (Color online) Particle identification using the time-of-flight between two MCPs. In blue are all events detected in the MCPs, the dashed, red line represents events in coincidence with a γ detection in the BGO array after software cuts. The abscissa represents the output amplitude of the time-to-amplitude converter. These data were taken during the measurement of the $E_{\mathrm{c.m.}} = 2.426$ MeV resonance.

charge states, a decrease in beam suppression of the separator was observed, due to ^{16}O beam in the same and next lower charge states being transmitted to the focal plane.

To determine the beam intensity, regular Faraday cup readings of the beam current were taken upstream and downstream of the target. While measuring the yield, the beam was monitored via the elastic scattering from the target into a silicon surface barrier detector mounted at 30° to the beam. Together, these data were used to normalize the beam intensity following the procedure outlined in Ref. [15]. The normalization factor R is calculated using the relation

$$R = \frac{I/q}{e}\frac{\Delta t}{N_\alpha}\frac{P}{E_{\mathrm{beam}}^2}\epsilon_{\mathrm{target}}, \tag{1}$$

where I is the beam current measured on the Faraday cup (FC), q is the charge state of the beam, e is the elementary charge, Δt is the time window during which the scattered α's were counted

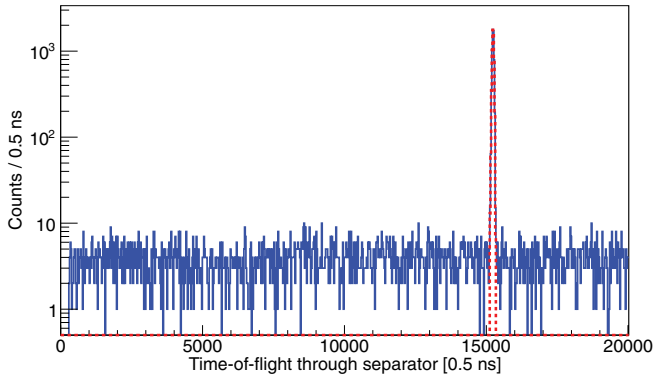

FIG. 4. (Color online) Particle identification using the time-of-flight through the separator. Since the TOF is tagged on the detection of a γ ray in the BGO array, it can only be applied to coincident events. The blue, solid line represents all coincident events, the red, dashed line represents events after software cuts. These data were taken during the measurement of the $E_{\mathrm{c.m.}} = 2.426$ MeV resonance.

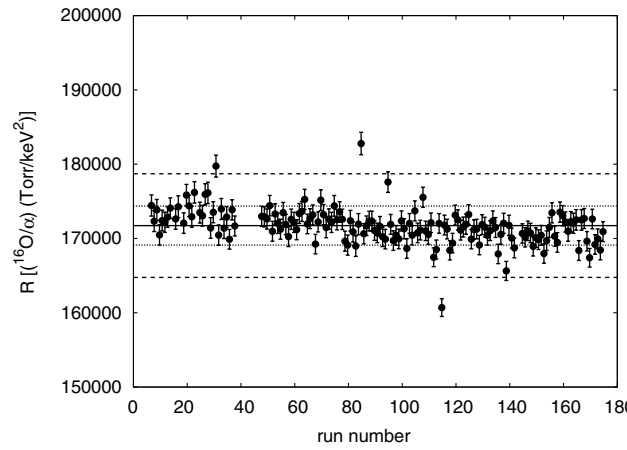

FIG. 5. Normalization factor R with statistical uncertainties for the measurements at $E_{\mathrm{c.m.}} = 1.694$ MeV in charge state 4^+. The solid line represents the average and the dotted line its statistical uncertainty. The dashed lines represent the total uncertainty, shown for comparison.

(60 s), N_α is the number of α particles scattered into the detector during Δt, P is the target pressure in torr, and E_{beam} is the beam energy per nucleon in keV. $\epsilon_{\mathrm{target}}$ is the transmission through the target, measured with an empty target, and limited mainly by the target entrance aperture. The uncertainty in the FC reading was 3%, the target pressure was known to 2%. The beam transmission through the target was measured to be $\epsilon_{\mathrm{target}} = 95(1)\%$. The normalization factors for the yield measurement runs at $E_{\mathrm{c.m.}} = 1.694$ MeV are shown in Fig. 5. From the integrated elastic scattering during all yield measurement runs, the total amount of beam on target was calculated.

Since both the separator transmission (via the recoil angle) and the efficiency of the BGO array, i.e., the probability of detecting at least one γ ray from a reaction, depend on the number of γ rays emitted in the reaction, the branching ratios of the decay had to be determined. To this end, GEANT3 simulations were performed assuming only a single mode of decay, and the resulting simulated γ spectra for each possible decay were together fitted to the measured ones. In the case encountered here the recoil angle was sufficiently small that the branching ratios had no influence on the separator transmission.

For a resonance whose width is narrow compared to the thickness of the target, the resonance strength $\omega\gamma$ can be calculated employing the relation [2]

$$Y(\infty) = \frac{\lambda^2}{2}\omega\gamma\frac{m_p + m_t}{m_p}\frac{1}{\epsilon}, \tag{2}$$

with Y the yield, λ the de Broglie wavelength, m_p and m_t the masses of the projectile and target, respectively, and ϵ the stopping power in the target gas. The stopping power was calculated using the measured energy loss across the target. This value has to be corrected for the finite target thickness using [16]

$$\frac{Y(\xi)}{Y(\infty)} = \frac{2}{\pi}\arctan\frac{\xi}{\Gamma}, \tag{3}$$

where ξ is the energy thickness of the target.

If the total width Γ of the resonance is known, the cross section on resonance can be calculated using

$$\sigma(E_R) = \frac{\lambda^2}{\pi}\frac{\omega\gamma}{\Gamma} \ . \tag{4}$$

In the case of nonresonant capture one can derive the cross section σ using [2]

$$Y = \sigma n \Delta x \ , \tag{5}$$

where n is the target density, and Δx the target thickness. The S factor is defined as

$$\sigma(E) = S(E)\frac{1}{E}e^{-2\pi\eta} \ , \tag{6}$$

where η is the Sommerfeld parameter.

III. ANALYSIS AND RESULTS

A. The 2.426 MeV resonance

For purposes of testing the complete experimental setup with a higher yield measurement, the reportedly well-studied 3^- resonance at $E_{\text{c.m.}} = 2.426$ MeV ([7,8]) was studied. The ^{16}O beam was accelerated to 768(1)A keV. The beam energy at the target exit was 753 A keV; the center-of-mass energy range covered by the target was 2.41 to 2.46 MeV. Given the resonance width of about 9 keV [7,8], the resonance was nearly fully inside the target. No indication of a γ transition contribution from the higher-lying 0^+ resonance ($\Gamma = 3.4(2)$ keV [17]) was found in the measured BGO detector hit pattern along the target as shown in Fig. 6. The beam intensity at the DRAGON target was on average 1.4×10^{12} s^{-1} and the total number of ^{16}O ions on target was $(1.04 \pm 0.003 \pm 0.06) \times 10^{17}$ (statistical and systematic uncertainty, respectively). The charge state fraction for 4^+ ions at this energy was measured to be 22(2)%. In this charge state, 5876 ^{20}Ne ions were identified in the focal plane detectors in coincidence with a γ event at the target. The maximum recoil cone angle of the ^{16}O$(\alpha,\gamma)^{20}$Ne reaction at this energy is 12 mrad for decay directly to the ground state. For other cascades, this angle is lowered on average due to the angular distribution of the γ rays. The observed γ transitions are shown in Fig. 7, where they are labeled a to e. Each of these

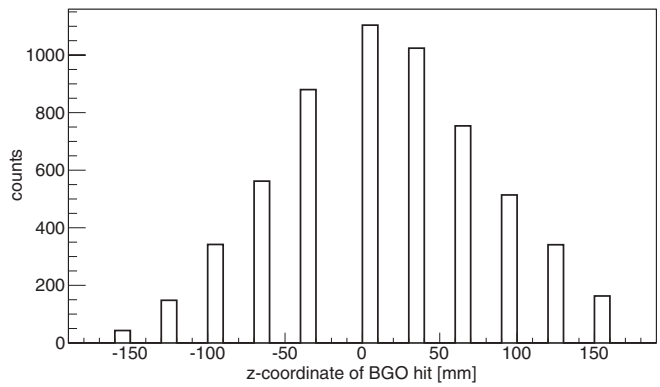

FIG. 6. BGO detector z coordinate hit pattern of the highest-energy recoil-coincident γ ray in the ^{16}O$(\alpha,\gamma)^{20}$Ne reaction at $E_{\text{c.m.}} = 2.426$ MeV. The beam enters the target from the left and exits at positive z values after losing energy in the target.

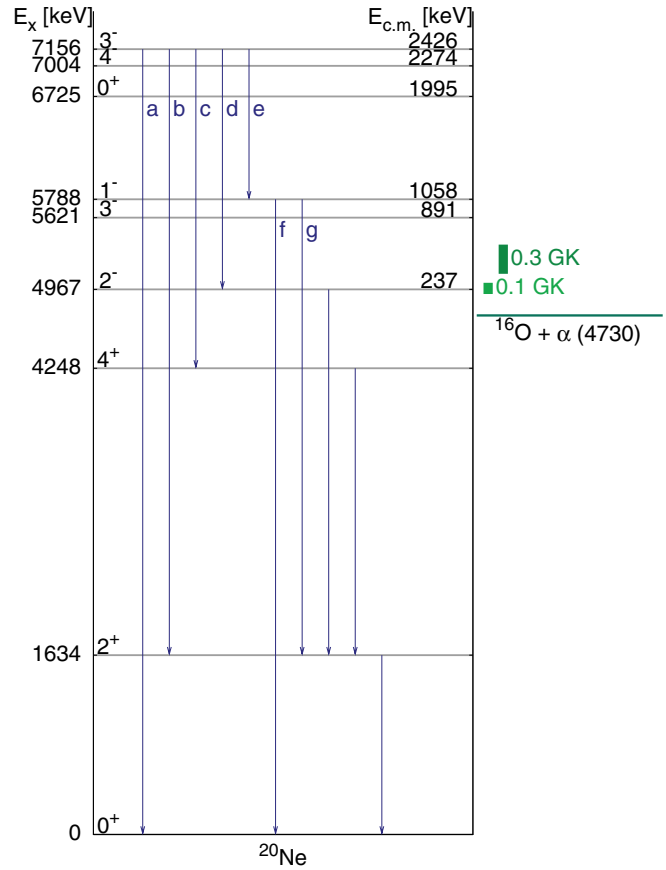

FIG. 7. (Color online) Decay scheme of the $E_{\text{c.m.}} = 2.426$ MeV resonance.

cascades was simulated separately in GEANT3. The resulting γ energy spectra were adjusted for the BGOs' combined energy resolution of about 24% at 661 keV. The branching ratios of transitions f and g from the $E_x = 5788$ keV level were taken from literature. The literature values for the branching ratios to the ground state [1,5,7,8,18] were averaged, and the combined cascade e was simulated with a branching ratio to the ground state of 21(2)%. For each cascade, 10000 events were simulated. The resulting simulated γ spectra were fitted to the measured ones. This was done within the ROOT data analysis framework using the TFractionFitter class which uses a standard likelihood fit with Poisson statistics to take into account statistical uncertainties both in the data and the simulation. The fitted spectrum is shown in Fig. 8, and the branching ratios are given in Table I. Compared to the previous branching ratio analyses our interpretation is significantly different and therefore included here although this resonance has little astrophysical significance.

While $E1$ transitions between $T = 0$ states in $N = Z$ nuclei are isospin suppressed [19], they are possible due to isospin mixing [20,21]. Cascade d in Fig. 7 from the 3^- state to the 2^- state at $E_x = 4967$ keV was not observed in previous experiments. While $M1$ transitions are usually expected to be weak compared to the $E1$ transitions, the above mentioned isospin suppression of $E1$ transitions can increase their importance. In the case of the 3^- level at $E_x = 5621$ keV in ^{20}Ne, decay to the 2^- level was observed, contributing

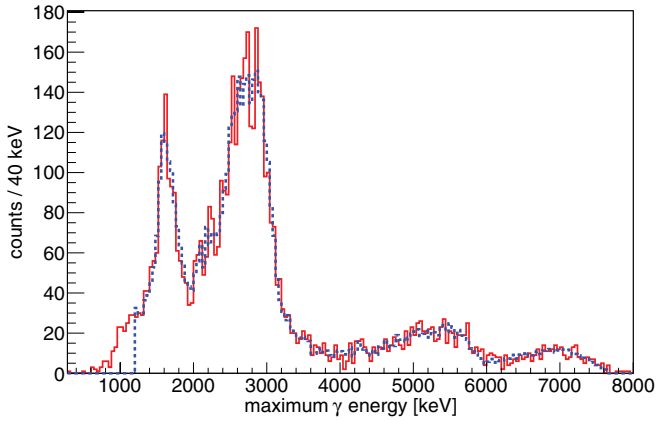

FIG. 8. (Color online) Energy of the most energetic γ ray per event for the measurement of the $E_{\mathrm{c.m.}} = 2.426$ MeV resonance; solid—measured, dashed—simulation.

4.8(16)% [18], 3.3(8)% [7], and 4.9(10)% [8]. For an $M1$ transition, the Weisskopf estimate scales with E_γ^3 [see Eq. (7) below], so it is conceivable that this transition plays a role also in the decay of this higher-lying resonance. The measured γ spectra for the decay of the $E_{\mathrm{c.m.}} = 2.426$ MeV resonance shown in Refs. [7,8] both display a peak at about 3.33 MeV, in agreement with decay from the $E_x = 4967$ keV state to the $E_x = 1634$ keV state. In Ref. [7], this line was attributed to contamination. Both spectra also show evidence of a line at 2.19 MeV, corresponding to a decay from the resonant 3^- state to the 2^- state. This line, however, lies on top of background lines, making its presence difficult to determine. Using the DRAGON separator, such background lines are suppressed, and including cascade d was found to be necessary to obtain a good fit to the measured spectrum.

Cascade e, on the other hand, has a large reported branching ratio in the literature [7,8,18], but in our measurement we were only able to set an upper limit of 3%. The 5788 keV state, which is the $K^\pi = 0^-$ band head [22], has a total width of $\Gamma = 28$ eV [17,22], and a γ width of $\Gamma_\gamma = 4.6 \times 10^{-3}$ eV [17]. It thus mainly α decays back to ^{16}O rather than decay through the γ transitions f and g. This explains why the 1368 keV transition from the resonance to the 5788 keV state is observed in both Refs. [7,8], while the decay of the 5788 keV level is not clearly visible in the spectra shown in either work. This is consistent with the measurement of MacArthur *et al.* [22], who observed the 1.368 MeV line, but no transitions from the 5788 keV state. Since the present work requires coincident detection of the ^{20}Ne recoil, the 1.368 MeV line is not observed.

Using the branching ratios given in Table I, the transmission through the separator and the BGO detection efficiency were determined from GEANT3 simulations. Both values barely changed when varying the branching ratios within their uncertainties; the BGO efficiency was found to be 83(3)%, and the separator transmission $99(^{+1}_{-2})$%. Thus, the reaction yield was calculated, and the resonance strength $\omega\gamma$ derived using Eqs. (2) and (3) with $\Gamma_{\mathrm{c.m.}} = 8.2 \pm 0.3$ keV from [17]. The resulting resonance strength is $\omega\gamma = (9.87 \pm 0.16 \pm 1.64)$ meV, which is lower than but consistent with the most recent literature values of (10.8 ± 1.5) meV [7], and (11 ± 1) meV [8].

Using this value for $\omega\gamma$, the radiative width Γ_γ was calculated via

$$\omega\gamma = \frac{(2J+1)}{(2j_p+1)(2j_t+1)} \frac{\Gamma_\alpha \Gamma_\gamma}{\Gamma}.$$

In this case, $J = 3$ for the resonance, $j_p = 0$ for the ^{16}O projectile, and $j_t = 0$ for the ^{4}He target. Since the total width Γ is far larger ($\Gamma_{\mathrm{c.m.}} = 8.2 \pm 0.3$ keV [17]) than the γ width Γ_γ, we use $\Gamma \approx \Gamma_\alpha$, and the terms effectively cancel. Thus, Γ_γ can be calculated to be $\Gamma_\gamma = 1.41 \pm 0.24$ meV. The contributions from the different cascades are listed in Table II. Using these values, the transition probabilities were compared to the Weisskopf estimates, which were calculated according to

$$\begin{aligned} E1: &\ \lambda\hbar = 6.8 \times 10^{-2} \cdot A^{2/3} E_\gamma^3, \\ E2: &\ \lambda\hbar = 4.9 \times 10^{-8} \cdot A^{4/3} E_\gamma^5, \\ E3: &\ \lambda\hbar = 2.3 \times 10^{-14} \cdot A^2 E_\gamma^7, \\ M1: &\ \lambda\hbar = 2.1 \times 10^{-2} \cdot E_\gamma^3 . \end{aligned} \tag{7}$$

The resulting partial width estimates are listed in Table III. The measured partial widths expressed in Weisskopf units are also given. All transitions are well below the recommended upper limits for γ-ray strengths [23]. Also listed in Table III are the values calculated by Mohr [3]. Mohr examined the reduced transition strength in the context of a two-body model, where ^{20}Ne has a dominating $^{16}\mathrm{O} \otimes \alpha$ cluster structure. The value calculated for cascade b shows relatively good agreement, even though in Ref. [3] no experimental value for this transition was known. For cascade d, the agreement is worse than with the previous experimental values taken from [17]. The values for cascade e cannot be compared, since the calculations in Ref. [3] refer only to the probability of γ decay to the 5788 keV level, while the present work includes the probability of subsequent γ decay from that level, which is essentially 0.

TABLE I. Branching ratios in % for the decay of the $E_{\mathrm{c.m.}} = 2.426$ MeV resonance. The labeling of the transitions corresponds to that in Fig. 7.

	E_x [keV]	this work	[18]	[7]	[8]
a	0	13(3)			6.2(1)
b	1634	16(4)			9.0(1)
c	4248	63(9)	60(5)	65.7(32)	54.4(16)
d	4967	8(4)			
e	5788	<3	40(5)	34.3(32)	30.4(4)

TABLE II. Partial resonance strengths and radiative widths for the different decay modes of the $E_{\mathrm{c.m.}} = 2.426$ MeV resonance. The labeling of the transitions corresponds to that in Fig. 7.

transition	E_x [keV]	$\omega\gamma$ [meV]	Γ_γ [meV]
a	0	1.28 ± 0.37	0.18 ± 0.05
b	1634	1.58 ± 0.47	0.23 ± 0.07
c	4248	6.22 ± 1.37	0.89 ± 0.20
d	4967	0.79 ± 0.42	0.11 ± 0.06
e	5788	<0.35	<0.05

TABLE III. Transition probabilities from the $E_x = 2426$ keV state in ^{20}Ne. Listed are the Weisskopf estimates, and the values in this work compared to the values calculated in Ref. [3]. The labeling of the transitions corresponds to that in Fig. 7.

	E_x [keV]	$E/M\mathcal{L}$	E_γ [MeV]	Weisskopf estimate [eV]	transition probability [W.u.] this work	Mohr [3]
a	0	*E*3	7.156	8.84×10^{-6}	20.7 ± 5.9	
b	1634	*E*1	5.522	84.36	$(2.67 \pm 0.80) \times 10^{-6}$	5.6×10^{-6}
c	4248	*E*1	2.908	12.32	$(7.21 \pm 1.58) \times 10^{-5}$	5.4×10^{-6}
d	4967	*M*1	2.189	0.22	$(5.12 \pm 2.70) \times 10^{-4}$	
e	5788	*E*2	1.368	1.27×10^{-5}	<4.5	41.6

Finally, the total S factor at this energy was calculated using Eqs. (4) and (6). The total width was again taken from [17], $\Gamma_{\text{c.m.}} = 8.2 \pm 0.3$ keV. The S factor was found to be $S(2.426\,\text{MeV}) = (78 \pm 1 \pm 13)$ MeVb, slightly lower than the R matrix calculation by Costantini *et al.* [1] $S(2.426\,\text{MeV}) = 107$ MeVb, as shown in Fig. 10 below. This discrepancy is due to the larger resonance strength $\omega\gamma = 11(1)$ meV from [8] and smaller width $\Gamma = 6.8(15)$ keV used in that study.

B. Direct capture at $E_{\text{c.m.}} = 1.694$ MeV

The cross section was measured at an energy of $E_{\text{c.m.}} = 1.694$ MeV, corresponding to $E_x = 6425$ keV. This energy was chosen as the S factor is close to the minimum between resonances (see, e.g., Fig. 12 from [1]), and the S_0 contribution of capture to the ground state was previously measured by Hahn *et al.* [5] at this energy.

The incoming ^{16}O beam had an energy of $538(1)A$ keV and after the gas target it was $520A$ keV, covering a center-of-mass range of 1.665–1.723 MeV. On average, the beam intensity at the DRAGON target was 1.8×10^{12} s^{-1}, with a total of $(9.21 \pm 0.02 \pm 0.50) \times 10^{17}$ ^{16}O nuclei incident on the gas target. The charge state fraction for 4^+ ^{20}Ne ions after the gas target was 35(2)%. The maximum cone angle of the reaction at this energy is 13 mrad for decay to the ground state in ^{20}Ne, thus fitting well into the acceptance of the DRAGON separator. The reaction at this energy proceeds either directly to the 0^+ ground state or via the 2^+ first excited state. A total of 551 ^{20}Ne nuclei could be identified in coincidence with BGO γ events.

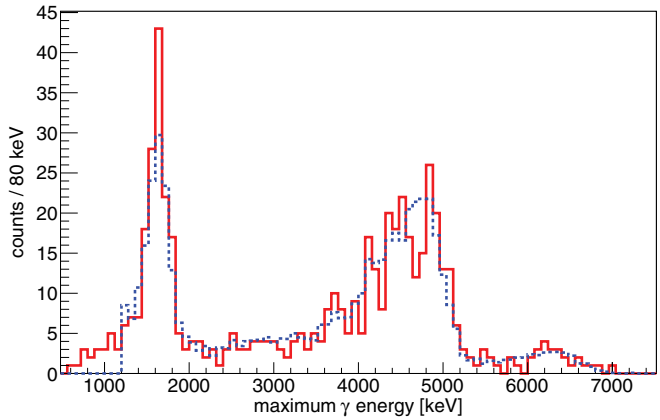

FIG. 9. (Color online) Energy of the most energetic γ ray per event for the measurement of the direct capture cross section at $E_{\text{c.m.}} = 1.69$ MeV; solid—measured, dashed—simulation.

The analysis of the data at this energy was carried out in the same way as for the $E_{\text{c.m.}} = 2.426$ MeV resonance; the S_0 (decay directly to the ground state) and S_2 (decay through the first excited state) contributions to the S factor were simulated separately, and together fitted to the measured BGO γ energy spectrum. The measured γ spectrum and the fitted combined simulation spectra are shown in Fig. 9. The resulting ratio is $S_2/S_{\text{tot}} = 89(5)\%$. Using this ratio, the transmission through the separator and the efficiency of the BGO array could again be determined from the simulations, and were found to be 97(2)% and 72(2)%, respectively. From the total number of ^{20}Ne recoils collected in coincidence with a γ ray in the BGO array the cross section σ was calculated again using Eq. (5). The resulting total S factor, Eq. (6) is $S_{\text{tot}}(1.694\,\text{MeV}) = (5.00 \pm 0.22 \pm 0.58)$ MeVb. This total S factor was then used together with the relative strength of the S_0 and S_2 contributions derived from the γ decay spectrum to calculate values for these contributions of $S_0 = (0.55 \pm 0.03 \pm 0.26)$ MeVb and $S_2 = (4.45 \pm 0.19 \pm 0.58)$ MeVb. Figure 10 compares these results to previous measurements. Good agreement is found for S_0 with the previous measurement by Hahn *et al.* [5] at this

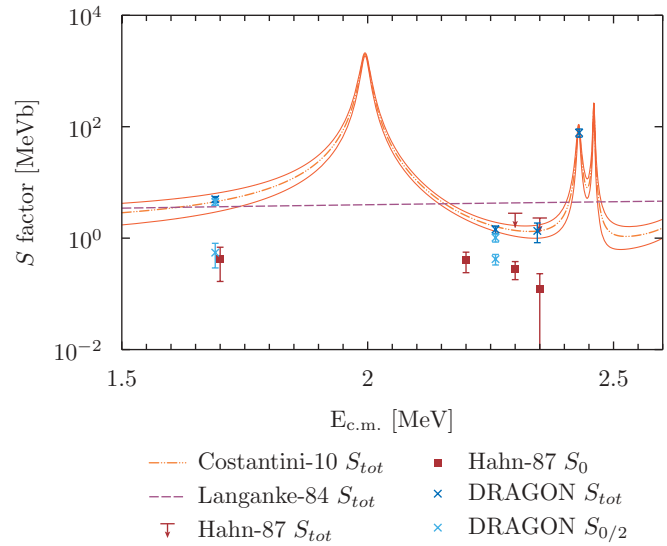

FIG. 10. (Color online) Comparison of this work to previous results: the total S factor given by Costantini *et al.* [1], Langanke [4], Hahn *et al.* [5], and the DRAGON results from the present work and [9]. Also shown are the upper limits by Hahn *et al.* for S_0. The points labeled 'DRAGON $S_{0/2}$' are the results presented here and in [9] for S_0 (lower value) and S_2 (larger value).

energy. Our value for the total S factor also agrees well with the R-matrix calculation performed by Costantini *et al.* [1]. Note that the data from [1] shown in Fig. 10 does not include their separately calculated contributions from the lower-lying 1^- resonance, which does not provide experimental yield at the energies investigated here.

C. S factor at $E_{\text{c.m.}} = 2.345$ MeV

An additional measurement was conducted at $E_{\text{c.m.}} = 2.345$ MeV, on the lower edge of the $E_{\text{c.m.}} = 2.426$ MeV resonance. At this energy, the reaction can still proceed through the tail of the $E_{\text{c.m.}} = 2.43$ MeV resonance. Due to low statistics (406 recoil events in coincidence) and the complicated γ spectrum at this energy, it was not possible to precisely determine branching ratios. However, the resonant contribution could be estimated to be $\approx$15(10)%. The S factor was determined to be $S(2.345\,\text{MeV}) = (1.35 \pm 0.07 \pm 0.51)$ MeVb.

IV. SUMMARY

We performed direct measurements of the total $^{16}O(\alpha,\gamma)^{20}Ne$ cross section. The measurement at $E_{\text{c.m.}} = 1.69$ MeV was the first direct measurement of the total S factor and both its components S_0 and S_2 at this low energy. Like our previous measurement at $E_{\text{c.m.}} = 2.26$ MeV [9], the observed S_0 contribution agrees well with the previous measurement by Hahn *et al.* [5]. Similarly, the total S factor agrees with the R-matrix calculation based predictions by Costantini *et al.* [1] and therefore provides experimental evidence for the validity of their reaction rate calculations. For the $E_{\text{c.m.}} = 2.43$ MeV 3^- resonance we find considerable disagreement with literature. MacArthur *et al.* [22] did not observe transitions to the ground state or first excited state, nor to the 4967 keV state. References [7,8,22] all observe strong feeding to the 5788 keV state, though Ref. [22] points out that this state α-decays. Our resulting resonance strength is thus somewhat smaller than the values given in Refs. [7,8] which seem to erroneously include the transition to that state.

ACKNOWLEDGMENTS

We would like to thank the beam delivery and ISAC operations groups at TRIUMF. The authors gratefully acknowledge funding from the Natural Sciences and Engineering Research Council of Canada. The Colorado School of Mines group was funded via Grant No. DE-FG02-93ER40789 from the US Department of Energy, Office of Nuclear Physics. We also gratefully acknowledge the invaluable assistance in beam production from K. Jayamanna.

[1] H. Costantini, R. J. deBoer, R. E. Azuma, M. Couder, J. Görres, J. W. Hammer, P. J. LeBlanc, H. Y. Lee, S. O'Brien, A. Palumbo *et al.*, Phys. Rev. C **82**, 035802 (2010).
[2] C. E. Rolfs and W. S. Rodney, *Cauldrons in the Cosmos* (The University of Chicago Press, Chicago, 1988).
[3] P. Mohr, Phys. Rev. C **72**, 035803 (2005).
[4] K. Langanke, Z. Phys. A **317**, 325 (1984).
[5] K. H. Hahn, K. H. Chang, T. R. Donoghue, and B. W. Filippone, Phys. Rev. C **36**, 892 (1987).
[6] D. Baye and P. Descouvemont, Phys. Rev. C **38**, 2463 (1988).
[7] H. Knee, Ph.D. thesis, Universität Stuttgart, Stuttgart, Germany, 1994.
[8] A. Mayer, Ph.D. thesis, Universität Stuttgart, Stuttgart, Germany, 2001.
[9] U. Hager, J. R. Brown, L. Buchmann, M. Carmona-Gallardo, L. Erikson, J. Fallis, U. Greife, D. Hutcheon, D. Ottewell, C. Ruiz *et al.*, Phys. Rev. C **84**, 022801(R) (2011).
[10] D. A. Hutcheon, S. Bishop, L. Buchmann, M. L. Chatterjee, A. A. Chen, J. M. D'Auria, S. Engel, D. Gigliotti, U. Greife, D. Hunter *et al.*, Nucl. Instrum. Methods Phys. Res. A **498**, 190 (2003).
[11] K. Jayamanna, Rev. Sci. Instrum. **81**, 02A331 (2010).
[12] L. Erikson, C. Ruiz, F. Ames, P. Bricault, L. Buchmann, A. A. Chen, J. Chen, H. Dare, B. Davids, C. Davis *et al.*, Phys. Rev. C **81**, 045808 (2010).
[13] C. Vockenhuber, L. Buchmann, J. Caggiano, A. Chen, J. D'Auria, C. Davis, U. Greife, A. Hussein, D. Hutcheon, D. Ottewell *et al.*, Nucl. Instrum. Methods Phys. Res. B **266**, 4167 (2008).
[14] C. Vockenhuber, L. Erikson, L. Buchmann, U. Greife, U. Hager, D. Hutcheon, M. Lamey, P. Machule, D. Ottewell, C. Ruiz *et al.*, Nucl. Instrum. Methods Phys. Res. A **603**, 372 (2009).
[15] J. M. D'Auria, R. E. Azuma, S. Bishop, L. Buchmann, M. L. Chatterjee, A. A. Chen, S. Engel, D. Gigliotti, U. Greife, D. Hunter *et al.*, Phys. Rev. C **69**, 065803 (2004).
[16] W. A. Fowler, C. C. Lauritsen, and T. Lauritsen, Rev. Mod. Phys. **20**, 236 (1948).
[17] D. R. Tilley, C. M. Cheves, J. H. Kelley, S. Raman, and H. R. Weller, Nucl. Phys. A **636**, 249 (1998).
[18] F. Ajzenberg-Selove, Nucl. Phys. A **475**, 1 (1987).
[19] L. A. Radicati, Phys. Rev. **87**, 521 (1952).
[20] P. Descouvement and D. Baye, Phys. Lett. B **127**, 286 (1983).
[21] P. Descouvemont and D. Baye, Nucl. Phys. A **459**, 374 (1986).
[22] J. D. MacArthur, H. C. Evans, J. R. Leslie, and H. B. Mak, Phys. Rev. C **22**, 356 (1980).
[23] P. M. Endt, At. Data Nucl. Data Tables **55**, 171 (1993).